JOURNAL OF Applied Polymer SCIENCE

Nanocomposites Based on Thermoplastic Polyurethane, Millable Polyurethane and Organoclay: Effect of Matrix Composition and Dynamic Vulcanization

Aruna Kumar Barick,[1,2] Young-Wook Chang[1]

[1]Polymer Nano Materials Laboratory, Department of Chemical Engineering, College of Engineering Sciences, Hanyang University, Ansan, Gyeonggi 426-791, Republic of Korea

[2]Research Institute of Engineering & Technology, Research Institute, Research Centers, Hanyang University, Ansan, Gyeonggi 426-791, Republic of Korea

Correspondence to: Y.-W. Chang (E-mail: ywchang@hanyang.ac.kr)

ABSTRACT: Dynamically vulcanized thermoplastic polyurethane (TPU)/millable polyurethane (MPU) blend nanocomposites, simple TPU/MPU blend nanocomposite, and TPU nanocomposite with 3 parts per hundred (phr) of organoclay were melt compounded in an internal mixer. Interfacial interactions between the organoclay and polyurethanes were examined by Fourier transform infrared spectroscopy, X-ray diffraction, and transmission electron microscope analysis, which revealed that the dispersion of organoclays significantly improved with increasing TPU content in the TPU/MPU blends and dynamic vulcanization process. Tensile test and dynamic mechanical analysis showed that the mechanical properties are improved with the TPU content in the TPU/MPU blends and dynamic vulcanization process. Both hardness and tension set of the samples decreased with increasing MPU content in the TPU/MPU blends. Thermal stability determined by thermo-gravimetric analysis revealed that it increased with increase in TPU concentration in the samples. Differential scanning calorimetry study showed that the glass transition temperature (T_g), melting temperature (T_m), and melt crystallization temperature (T_c) of the samples were significantly affected by the blend composition and dynamic vulcanization. Dynamic melt rheology of the nanocomposite samples in the molten state revealed a pseudo solid-like behavior as well as an enhanced shear thinning behavior, and the variation of the rheological properties are well correlated with blend compositions and morphology of the nanocomposites. © 2013 Wiley Periodicals, Inc. J. Appl. Polym. Sci. 000: 000–000, 2013

KEYWORDS: clay; mechanical properties; polyurethanes; blends; composites

Received 19 February 2013; accepted 13 June 2013; Published online 00 Month 2013

DOI: 10.1002/app.39670

INTRODUCTION

Polymer/clay nanocomposites (PCN) have created a center of interest in the recent decades because the materials properties are enhanced by many folds relatively at very minute nanofiller loading in comparison with the conventional micro-fillers.[1] The chemical modifications of clay using exchangeable cations makes it organophilic or hydrophobic as well as enhances the interlayer or gallery spacing; as a result the polymer backbone molecular chains are easily inserted into the gallery spacing, leading to exfoliation and homogeneous dispersion of clays within polymer matrix. It is reported that the performance properties such as modulus and strength, thermal stability, gas permeability, flame retardancy, chemical resistance, etc. of PCN are remarkably enhanced by incorporation of clay.[2]

Preparation of PCN via melt intercalation technique using conventional high shear mixing machine have been considered as the most promising approach that greatly improved the commercial aspects in term of easiness and cost.[3] The most driving force for homogeneous dispersion of clays within the polymer matrix is the appropriate melt viscosity, where the polymer molecular chains are successfully diffused into the clay galleries under a suitable shear stress, which is further supported by the strong affinity of polymer matrix and clay for each other. Moreover, the polar polymer matrix forms a strong interphase interaction with clay surface through hydrogen bonding, achieving a very high degree of exfoliation.[4]

Thermoplastic elastomer (TPE) is a special type of polymer blend system possessing continuous melt processability of thermoplastics with flexibility and low-modulus properties of elastomers. The TPE materials continue to grow in a wide variety of applications mainly automotive industry in last decades. Dynamically vulcanized thermoplastic/rubber blend, often called

a thermoplastic vulcanizate (TPV), is an important class of TPE. The rubber phase is selectively vulcanized in TPV by the addition of suitable curing agents during melt mixing of a thermoplastic and a rubber. The vulcanized particulate rubber phase is homogeneously dispersed within the continuous thermoplastic phase by the dynamic vulcanization process and thus can exhibit rubber-like properties and melt processability like thermoplastics.[5] The TPV can be effectively manufactured by proper combination of thermoplastics and rubbers. Properties of the TPVs strongly depend on the composition of the constituent polymers, extent of crosslinking in rubber phase, and degree of dispersion and particle size distribution of dispersed rubber phase.[6–8]

Studies on TPV/clay nanocomposites (TPVCN) have been widely reported in literature.[9–18] Nanostructured TPVCN can be fabricated by melt mixing method using proper modification of nanofillers and matrix polymers to impart sufficient thermodynamic compatibility between them. The TPVCN can exhibit excellent recyclability, melt processability, and performance properties. Thus, TPVCN is successfully employed in diverse applications such as electrical, construction, healthcare, packaging, and many more fields. The literature review revealed that some published papers are dedicated to the polypropylene/ethylene propylene diene monomer rubber (PP/EPDM),[9–17] and ethylene vinyl acetate/natural rubber ((EVA/NR)[17] blends based TPVCN.

Polyurethane elastomers are important class of polymer materials, which has diverse applications including footwear, automotive, hose and belting, marine and oil field products, and other things. Polyurethane elastomers can be divided into two different types depending upon the structure i.e. thermoplastic polyurethane (TPU) and millable polyurethane (MPU). The MPU is a rubber like gum, which is generally compounded by means of conventional rubber processing equipments in the presence of other ingredients/additives. The MPU vulcanizates offer a combination of physical properties such as high tensile and tear strength, outstanding abrasion resistance, oil and fuel resistance, ozone and environment protection, and good dynamic load bearing and damping properties, which is not found in natural or synthetic rubbers. As a comparison, TPU possesses all above properties along with the high hydrolytic resistance, resistance to weak acids/bases, paintability, best low temperature flexibility, resistance to microbial biodegradation, high impact strength, and excellent melt processability. Hence, the overall material properties of the TPU/MPU blend can be improved due to the synergistic effect imparted by the individual components.

The literature survey reported that an ample number of research and development have been conducted regarding blends of TPU with different rubbers, which include the blend of TPU with NR,[19–21] epoxidized NR (ENR),[22] EPDM rubber,[23,24] nitrile butadiene rubber (NBR),[25,26] carboxylated NBR (XNBR),[27,28] polydimethyl siloxane (PDMS) rubber,[29–31] styrene butadiene styrene (SBS) rubber,[32] and methyl vinyl silicone (MVS) rubber.[33] Mishra et al. have studied the effect of nanofiller on the heat shrinkable behavior and mechanical properties of low density polyethylene (LDPE)/MPU/organoclay ternary blend nanocomposites.[34] The literature survey showed that the properties of TPU/MPU blend system have not been studied yet.

In the present article, we prepared dynamically vulcanized TPU/MPU blends/organoclay nanocomposites (DV-TPUMPUCN), simple TPU/MPU blend/organoclay nanocomposites (TPUMPUCN), and TPU/organoclay nanocomposites (TPUCN) by a melt compounding process. Effects of blend compositions and dynamic vulcanization process on the properties of TPU/MPU blends and their nanocomposites with organoclay were examined. The main aim of the current research is to prepare low hardness TPU material with good damping properties and acceptable mechanical strength for some applications.

Table I. Compounding Formulations of Samples

Sample code	TPU	MPU	C30B	DCP	TAC
$T_{25}M_{75}C_3V$	25	75	3	6	2
$T_{50}M_{50}C_3V$	50	50	3	6	2
$T_{75}M_{25}C_3V$	75	25	3	6	2
$T_{100}M_0C_3U$	100	0	3	0	0
$T_{50}M_{50}C_3U$	50	50	3	0	0

EXPERIMENTAL

Materials

Polyether based TPU elastomer (Neothane® 6185A) with Shore hardness of 86 ± 2A and density of 1.12 gm/cm^3 was purchased from Dongsung Highchem, South Korea. Peroxide curable polyether based MPU elastomer (Millathane® E40) was procured from the TSE Industries, USA. It has density of 1.07 gm/cm^3 and Mooney viscosity of 30–60 $ML_{(1+4)}$ at 100°C. Cloisite® 30B (C30B), an organically modified montmorillonite (OMMT) was supplied by Southern Clay, USA Products having CEC of 90 meq/100 gm and methyl tallow *bis*−2-hydroxyethyl quaternary ammonium (MT2EtOH) as organic modifier with tallow composition of ∼65% C18; ∼30% C16; ∼5% C14. Dicumyl peroxide (DCP) used as peroxide curing agent having molecular weight of 270.37, density of 1.56 gm/mL at 25°C, melting point in the range of 39–41°C, and decomposition temperature of 90°C was acquired from Sigma-Aldrich, USA. The triallyl cyanurate (TAC) used as coagent for the peroxide curing system having molecular weight of 249.27, density of 1.11 gm/cm^3 at 30°C, and melting point in the range of 26–28°C was sold by Tokyo Chemical Industry, Japan.

Preparation of Samples

TPU and C30B were dried under vacuum (30" Hg) at 50°C for 24 h before use. The samples were prepared by melt blending in an internal mixer (Haake Polylab System, USA) equipped with a cam rotor using a rotor speed of 60 rpm and at a temperature of 180°C for 6 min, which was optimized in our previous work using the statistical methods.[35] Firstly, the TPU was added into the mixing chamber and kept for a while to make it soften. Secondly, the MPU and organoclay were added followed by addition of curatives. The amount of organoclay was 3 phr. The obtained compounds were compression molded into test pieces. The compositions of the samples are shown in Table I. "T" and

"M" in the sample designations denotes TPU and MPU, respectively. The sample designations having "V" at the end denote dynamically vulcanized samples and those having "U" at the end denote simple blended samples in which dynamic vulcanization was not employed, and the "C" in the sample designations denotes the organoclay (C30B).

Measurement and Characterizations

Fourier transform infrared (FTIR) spectrophotometer (Nicolet 6700, Thermo Fisher Scientific, USA) equipped with an attenuated total reflectance (ATR) accessory was used to evaluate the interfacial interaction between organoclay and polyurethane matrices. The surface of the compression molded samples was taken for FTIR study. FTIR spectra were recorded in the dispersive mode within a range of 400–4000 cm^{-1} at a resolution of 4 cm^{-1} and 16 scans were collected for each trace. Change in the gallery distance of the organoclays was examined using X-ray diffraction (XRD) patterns recorded on a X-ray diffractometer (D/MAX-2500/PC, Rigaku Corporation, Japan) with a Cu-$K_{\alpha 1}$ ($\lambda = 0.154$ nm) radiation source at a generator voltage of 40 kV and a current of 100 mA. The compression molded samples of 1×1 $inch^2$ was taken for XRD study. The data were obtained from $2\theta = 1° - 10°$ at a scanning speed of 2°/min. Dispersibility of the silicate layers in the samples was evaluated using transmission electron microscope (TEM) (JEM-2100F, JEOL, Japan). TEM micrographs were obtained using an acceleration voltage of 200 kV. The cryoultramicrotome (PT-PC PowerTome Ultramicrotomes, Boeckeler Instruments, USA) was employed for the preparation of ultra-thin sections of <100 nm thickness from the compression molded sample sheets at an ambient temperature of around −80°C [well below the glass transition temperature (T_g) of the polymer] with the help of diamond knife. Tensile properties were measured as per the ASTM D-412-98 procedure using a universal testing machine (UTM) (STM-10E, United Calibration, USA) at 25°C with a crosshead speed of 50 mm/min. The tensile test samples were prepared by specimen preparation machine. Five dog-bone shaped samples were used for each composition of samples. The hardness of the samples was measured by durometer hardness tester (GS-702N, Teclock, Japan) according to the ASTM D-2240D standard procedure. Dynamic storage modulus of the samples was measured using a dynamic mechanical analyzer (Q800, TA Instruments, USA). The sample was subjected to a cyclic tensile strain with amplitude of 10 μm and a frequency of 1 Hz. The temperature was increased from −100 to 225°C at a heating rate of 2°C/min. The thermal stability of the samples were studied using thermogravimetric analysis (TGA) (SDT 2960, TA Instruments, USA) by taking 10 ± 1.5 mg samples at a heating rate of 10°C/min under nitrogen atmosphere with a flow rate of 50 mL/min. The T_g, T_m, and T_c of the samples were determined by using a differential scanning calorimetry (DSC) (DSC 2010, TA Instruments, USA) in the liquid nitrogen atmosphere by taking 5.0 ± 1.5 mg of sample for each composition. The samples were first heated from room temperature to 250°C at a scan rate of 10°C/min and then kept at 250°C for 10 min to remove the previous thermal history and to obtain a clearer T_g, followed by cooling to −100°C with the same scan rate to measure T_c. Finally, the sample was reheated from −100 to 250°C at a scan rate of 10°C/min to measure the T_g and T_m. Melt rheological behavior of the samples were measured by advanced rheometric expansion system (ARES) (Rheometrics, USA) using a set of 25 mm diameter parallel plates with a sample of 1–2 mm thickness, under the continuous purge of dry nitrogen in order to avoid the degradation of samples. The test was carried out within the frequency range of $10^{-1}-10^{2}$ rad/s at a temperature of 180°C with an applied strain of 10% that reside well within the linear viscoelastic region.

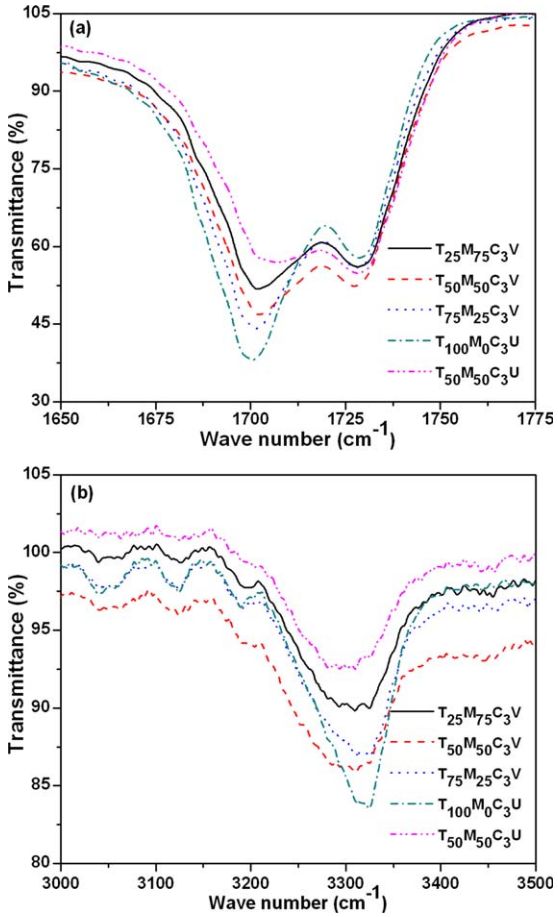

Figure 1. FTIR spectra of (a) carbonyl and (b) amine bond stretching regions of samples. [Color figure can be viewed in the online issue, which is available at wileyonlinelibrary.com.]

RESULTS AND DISCUSSION

FTIR Analysis

FTIR spectra of all samples in the carbonyl (>C—O) and amine (—NH—) stretching regions are presented in Figure 1(a,b). Figure 1a shows the absorption peaks at around 1729 and 1701 cm^{-1}, which are assigned to free and hydrogen bonded >C═O stretching vibrations, respectively. This indicates that the hydrogen bonding interactions occurred between the >C═O groups of urethane linkage and hydroxyl (—OH) groups exist on the surface of organoclay in all samples.[36] It is noted that the organoclay more effectively restricts the segmental mobility of hard domains in comparison with the soft domains of polyurethane matrix, which results in reduction of inter- and intramolecular hydrogen bonds among hard segments of polyurethane

matrix.[37] It can be seen from the spectra that the area under the hydrogen bonded absorption peak increased with increasing TPU content in the samples and the peak position shifted to higher wave length, which revealed that the hydrogen bonding interactions become more prominent with increasing TPU content in the samples. When compared the FTIR spectrum of $T_{50}M_{50}C_3U$ and $T_{50}M_{50}C_3V$, the hydrogen bonding interactions is more pronounced in dynamically vulcanized TPU/MPU blend nanocomposites.

Figure 1(b) shows FTIR spectra in the —NH— stretching vibration region, which showed a broad absorption peak centered at around 3308 cm^{-1}, that attributed to the stretching vibration of hydrogen bonded —NH— groups of urethane linkage. The peak corresponding to the free —NH— group stretching vibration, which appears at around 3450 cm^{-1}, almost disappeared. This indicates that all —NH— groups present in polyurethane matrix participated in the hydrogen bonding interactions with —OH group on the surface of the organoclay.[38] The area associated with the absorption peak corresponding to the hydrogen bonded —NH— group increased with increasing TPU content in the samples and become prominent in dynamically vulcanized samples. These trends are in good accordance to the variations of hydrogen bonded carbonyl absorption peak as observed in Figure 1(a). On the basis of FTIR results, it can be concluded that the interfacial interactions between the polyurethane matrices and organoclay increased with TPU content in the TPU/MPU blend nanocomposites and by dynamic vulcanization process as well.

XRD Analysis

Figure 2 shows the XRD patterns of organoclay (C30B) and all nanocomposite samples. The neat C30B shows an intense diffraction peak centered at $2\theta = 4.78°$ and a small broad peak at $2\theta = 9.56°$ corresponds to the basal spacing of 1.8472 and 0.9244 nm of d_{001} and d_{002} Bragg reflection planes, respectively.[39] The strong diffraction peak disappears in the XRD pattern of the nanocomposite samples. These observations imply that the polymer chains are intercalated between the layers of organoclay and induce delamination of the organoclays, which resulted in high disordered nanoscale dispersion of the organoclay throughout the TPU/MPU blend matrix.[40] Homogeneous dispersion of C30B within polyurethane matrix is attributed to the presence of strong hydrogen bonding interactions between >C═O groups of polyurethane and —OH groups in C30B organoclays.[41] It can be seen in Figure 2 that the intensity of the XRD lines decreased with TPU content in the samples and the intensity is lowest in TPU nanocomposite, which implied that the TPU content in the samples may affect the degree of intercalation of the polymer chains between the layers of the organoclays. From the FTIR observation as discussed above, the hydrogen bonding interactions between polyurethane chains and the organoclay increased with TPU content in the samples. This result can be interrelated with the variation of the intensity, i.e., as TPU content in the MPU/TPU blend is higher, the affinity of the matrix polymer with organoclay increased, thereby the higher intercalation occurred. It can also be noted from Figure 2 that the unvulcanized TPU/MPU blend based nanocomposite ($T_{50}M_{50}C_3U$) shows a broad peak, while the dynamically vulcanized TPU/MPU blend based nanocomposite ($T_{50}M_{50}C_3V$) does not show any peaks. This indicates that the dynamic vulcanization can facilitate the intercalation of the polymer chains into the layers of the organoclay, probably because the stronger shearing action can be exerted onto the layers of the organoclay due to dynamic vulcanization and induced the delamination of the organoclays in the polymer matrix. On the basis of these observations, it can be inferred that the degree of delamination of the organoclays in the polymer matrix are dependent on the degree of shear during the melt mixing as well as the affinity of matrix polymer chains with the surface of an organoclay.

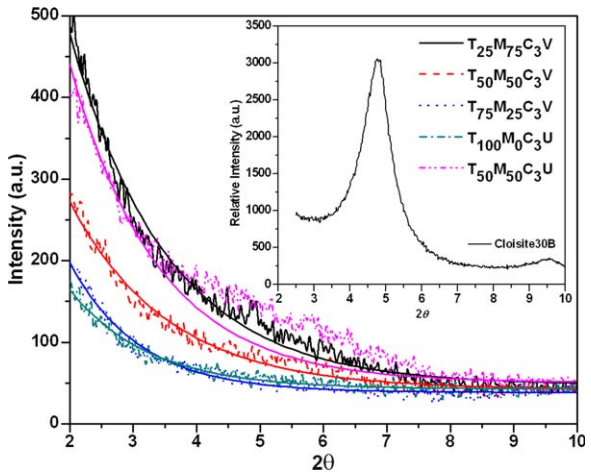

Figure 2. XRD patterns of samples. [Color figure can be viewed in the online issue, which is available at wileyonlinelibrary.com.]

Morphology

Figure 3(a–e) represents the TEM microphotographs of the ultrathin sections of the compression molded samples. The dark lines in Figure 3(a–e) are the cross-sections of the clay layers. It can be seen in Figure 3(a–c) that the degree of dispersion of the organoclays improved with increasing TPU content in the samples. In the sample with lowest TPU content ($T_{25}M_{75}C_3V$), several agglomerated particles are observed, while these are not seen in the sample with highest TPU content ($T_{75}M_{25}C_3V$) instead the clay nanolayers with 10–30 nm thickness were uniformly dispersed in the polyurethane matrix. Similar nanostructured morphology was observed in TPU nanocomposite [Figure 3(d)]. This trend is in good agreement with both XRD and FTIR results. The TPU has a higher affinity with organoclays than the MPU, and thereby more facile intercalations of polymer chains and consequently delamination of the silicate layers of the organoclays occurred with increasing TPU content in the TPU/MPU blend matrix. When compared the TEM results of $T_{50}M_{50}C_3U$ and $T_{50}M_{50}C_3V$ as shown in Figure 3(c,e), respectively, the organoclays are more uniformly dispersed within the dynamically vulcanized TPU/MPU blend matrix than that of simple TPU/MPU blend matrix. This is also in good agreement with XRD results. As discussed earlier, the dynamic vulcanization process produced high shearing force during melt mixing process, which induced delamination of the organoclay.[3,4]

Mechanical Properties

Typical representative stress–strain curves of all samples are shown in Figure 4 and the tensile strength, elongation at break,

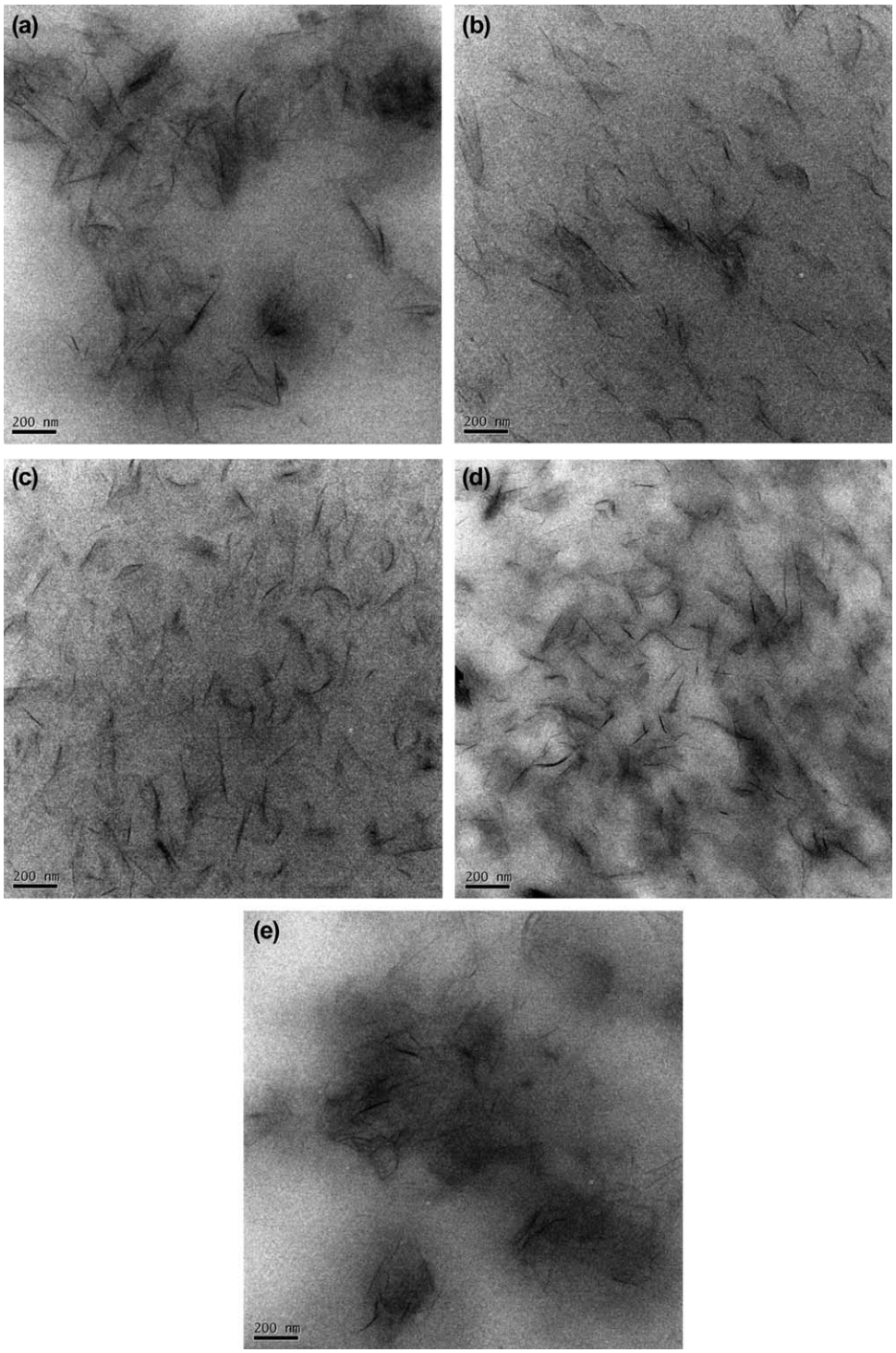

Figure 3. TEM micrographs of samples (a) $T_{25}M_{75}C_3V$, (b) $T_{50}M_{50}C_3V$, (c) $T_{75}M_{25}C_3V$, (d) $T_{100}M_0C_3U$, and (e) $T_{50}M_{50}C_3U$.

modulus at 100% elongation, and Young's modulus are represented in Table II. It can be observed that the dynamically vulcanized TPU/MPU blend nanocomposites showed lower tensile strength and elongation at break as compare to TPU nanocomposite ($T_{100}M_0C_3U$), because addition of MPU rubbery phase causes disruption of small range regular ordered structure of hard segments as well as imposes restriction on the molecular chain mobility of soft segments in TPU matrix.[22] In the case of dynamically vulcanized TPU/MPU blend nanocomposites, the tensile strength, elongation at break, modulus at 100% elongation, and Young's modulus increased with an increase in TPU content, which indicates higher stiffness of TPU as compared to MPU as well as higher affinity of the TPU with the organoclay than that of the MPU. It can also be seen that the dynamically

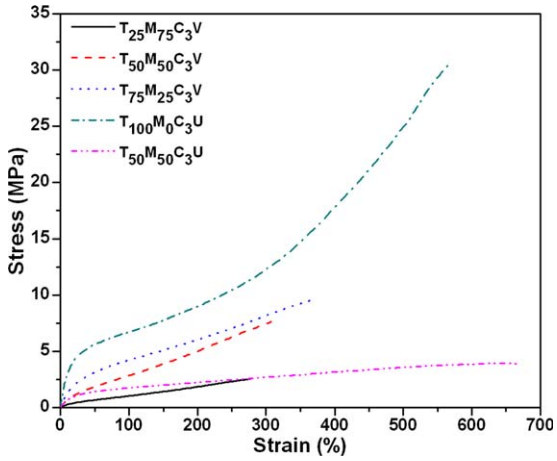

Figure 4. Tensile stress–strain plots of samples. [Color figure can be viewed in the online issue, which is available at wileyonlinelibrary.com.]

vulcanized TPU/MPU blend nanocomposite ($T_{50}M_{50}C_3V$) showed higher tensile properties than the simple TPU/MPU blend nanocomposite ($T_{50}M_{50}C_3U$), which implies that the dynamic vulcanization process accelerated the improvement of tensile strength and modulus. This is due to finer dispersion of organoclay layers and possible compatibilization of TPU/MPU blends during dynamic vulcanization process.[42] It can be seen from Table II that the dynamically vulcanized TPU/MPU blend nanocomposites exhibit lower tension set values (higher permanent set) than that of the TPU nanocomposite, implying significant increase in elasticity with MPU content. It is also observed that the tension set of the dynamically cured $T_{50}M_{50}C_3V$ is substantially reduced than the simple $T_{50}M_{50}C_3U$ blend nanocomposite because the former shows vulcanized MPU particulate phase dispersed in TPU matrix, while the latter shows dual cocontinuous phase of TPU/MPU blend matrix.[43] As shown in Table II, the hardness of the dynamically cured TPU/MPU blend nanocomposites decreased with increase in proportion of MPU, which indicates higher elasticity or softness of the samples with higher MPU content. The hardness of dynamically cured $T_{50}M_{50}C_3V$ sample is higher than the simple $T_{50}M_{50}C_3U$ sample due to the difference in morphological properties of the TPU/MPU blend matrix.[22]

Dynamic Mechanical Properties

Temperature dependence of storage modulus (E') for samples is shown in Figure 5(a) and the storage modulus at 30 and −30°C are tabulated in Table III. It is observed from Figure 5 that there is a large drop in storage modulus at around −26 to −34°C

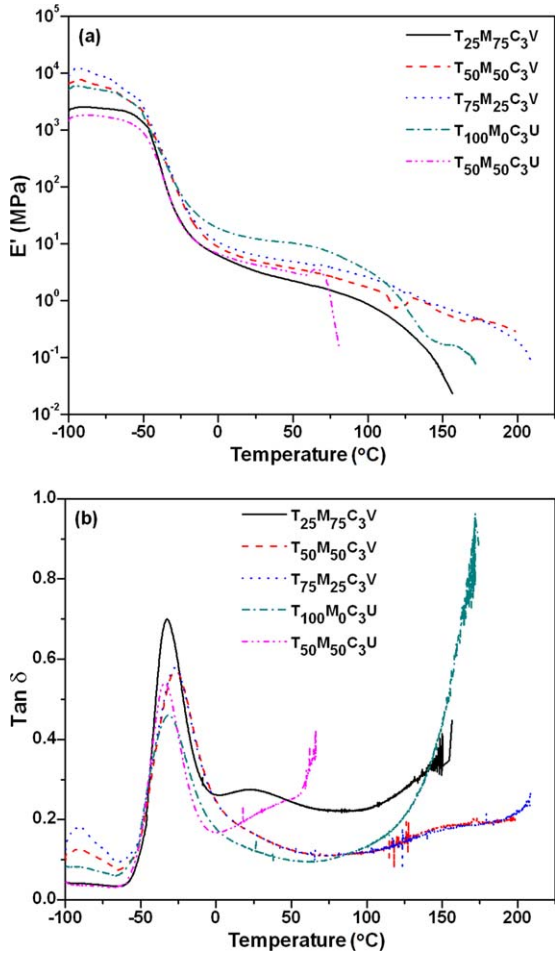

Figure 5. Temperature dependence of dynamic storage modulus (E') of samples. [Color figure can be viewed in the online issue, which is available at wileyonlinelibrary.com.]

corresponding to the glass transition of the TPU/MPU blend matrix, and then formed a plateau region at which the modulus kept quite stable up to about 100°C or more corresponding to the melting transition of the hard segment of TPU. It can be seen that the storage modulus at the rubbery plateau region increased with an increasing TPU content in the dynamically vulcanized TPU/MPU blend nanocomposites. It can also be seen that $T_{50}M_{50}C_3V$ showed higher modulus than the $T_{50}M_{50}C_3U$. The trend is in good accordance to the mechanical properties.

The dynamic mechanical analysis (DMA) thermograms of all samples for temperature dependence on damping factor (tan δ)

Table II. Mechanical Properties of Samples

Sample code	Tensile strength (MPa)	Elongation at break (%)	Modulus at 100% elongation (MPa)	Young's modulus (MPa)	Tension set (%)	Hardness (Shore A)
$T_{25}M_{75}C_3V$	2.54	277	1.02	2.40	1.25	50
$T_{50}M_{50}C_3V$	7.61	308	2.83	6.11	2.50	75
$T_{75}M_{25}C_3V$	9.55	370	4.21	12.53	5.83	85
$T_{100}M_0C_3U$	30.44	566	6.71	28.31	10.50	90
$T_{50}M_{50}C_3U$	3.85	666	1.74	6.40	7.50	65

Table III. DMA Data of Samples

Sample code	E' at 30°C (MPa)	E'' at 30°C (MPa)	T_g from tan δ peak (°C)
$T_{25}M_{75}C_3V$	44.80	3.00	−32.2
$T_{50}M_{50}C_3V$	126.7	4.63	−26.6
$T_{75}M_{25}C_3V$	142.8	5.86	−27.2
$T_{100}M_0C_3U$	136.0	11.66	−32.3
$T_{50}M_{50}C_3U$	44.85	4.00	−34.0

are expressed in Figure 5(b). The protruding broad peaks in the temperature range of −50 to 0°C are defined as the second order dynamic glass transition of the soft segments of TPU/MPU blend matrix. As shown in Table III, the tan δ peak temperature of the dynamically cured TPU/MPU blend nanocomposites shifted to higher temperature than the TPU nanocomposite, which is caused due to the rigid crosslinked network structures formed by the dynamic vulcanization process accompanied with the stiffening effect employed by the rigid organoclays. The shifting of T_g to higher values in case of dynamically vulcanized TPU/MPU blend nanocomposites as compared to TPU nanocomposite, also informed the strong compatibility between TPU and MPU phases. The $T_{50}M_{50}C_3U$ exhibited the tan δ peak temperature at about −34°C that is well below the tan δ peak temperature of $T_{50}M_{50}C_3V$, which implied that there is more rubber characteristic in the former case that is due to the lack of any stable structures. The half width at half maximum (HWHM) of the tan δ curves is largest for dynamic vulcanized samples, hence performing better damping behavior or elastic response as compared to both simple TPU/MPU blend nanocomposites and TPU nanocomposite, resulted from the more energy absorption and dissipation capability of the vulcanized particulate dispersed MPU phase. The peak height of the TPU nanocomposites is lowest, which indicated lowest elastic behavior. As shown in Figure 5(b), the values of tan δ always resided well below the unit that informed good damping behavior for all samples.

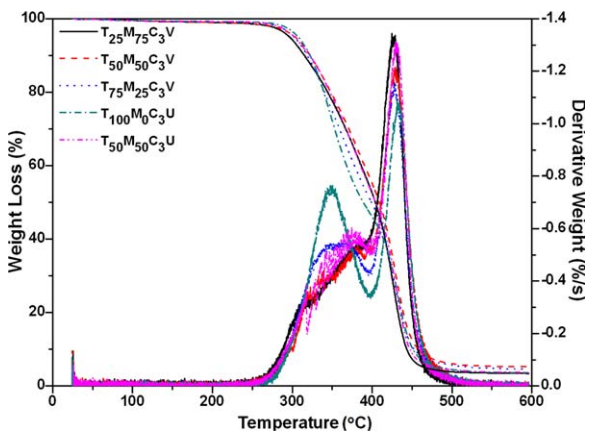

Figure 6. TGA and DTG thermograms of samples. [Color figure can be viewed in the online issue, which is available at wileyonlinelibrary.com.]

Table IV. TGA Data of Samples

Sample code	$T_{5\ wt\ \%}$ (°C)	$T_{50\ wt\ \%}$ (°C)	$T_{p(hard)}$ (°C)	$T_{p(soft)}$ (°C)
$T_{25}M_{75}C_3V$	297	404	-	427
$T_{50}M_{50}C_3V$	304	409	381	430
$T_{75}M_{25}C_3V$	303	399	356	428
$T_{100}M_0C_3U$	307	389	348	432
$T_{50}M_{50}C_3U$	303	404	378	430

$T_{5\ wt\ \%}$, temperature at 5 wt % weight loss; $T_{50\ wt\ \%}$, temperature at 50 wt % weight loss; $T_{p(hard)}$, temperature at first maximum degradation rate peak; and $T_{p(soft)}$, temperature at second maximum degradation rate peak.

Thermal Stability

The TGA and DTG (derivative thermo-gravimetric) thermograms of samples are shown in Figure 6 and data are presented in Table IV. The thermal degradation of polyurethane matrix takes place at two stages; the lower temperature derivative peak in between 300 and 400°C is due to the thermal decomposition of hard segments and higher temperature derivative peak ranging from 400 to 450°C is assigned to the thermal degradation of soft segments.[44] The TPU nanocomposite shows a large peak corresponds to the degradation of hard segments, while the peaks for dynamic vulcanized TPU/MPU blend nanocomposites are significantly diminished and shifted to higher temperature, which confirmed that the rate of degradation is controlled by the development of highly crosslinked polymeric network structures. The soft segment degradation is almost retained with increase in TPU matrix content, which may be due to the strong adhesion bonding between TPU and organoclays as well as homogeneous dispersion of organoclays within the TPU matrix. It is concluded that the incorporation of organoclay entered into both hard and soft segments of the TPU/MPU blend matrix. The thermal stability of $T_{50}M_{50}C_3V$ is slightly higher than the $T_{50}M_{50}C_3U$.

Thermal Properties

The DSC thermograms for second heating cycle of samples are displayed in Figure 7(a). The curves showed a prominent second order thermal transition in between −75 and −25°C due to change in heat capacity (ΔC_p), which corresponds to the T_g of the soft segment ($T_{g(soft)}$) of the TPU/MPU blend matrix. The position of the $T_{g(soft)}$ gradually increased with increase in proportion of TPU matrix i.e., the reinforcing effect imparted by the organoclay occurs more within the TPU matrix than the MPU matrix as well as the amorphous content decreased with increasing TPU loading. The $T_{g(soft)}$ position shifted to a higher temperature for dynamically cured TPU/MPU blend nanocomposite ($T_{50}M_{50}C_3V$) than that of simple TPU/MPU blend nanocomposite ($T_{50}M_{50}C_3U$), because the highly dense network structures formed by the dynamic vulcanization process successfully restricted the segmental mobility of the molecular back bone chains of polyurethanes.

The thermograms shown in Figure 7(a) for TPU nanocomposite ($T_{100}M_0C_3U$) showed a prominent broad endothermic peak

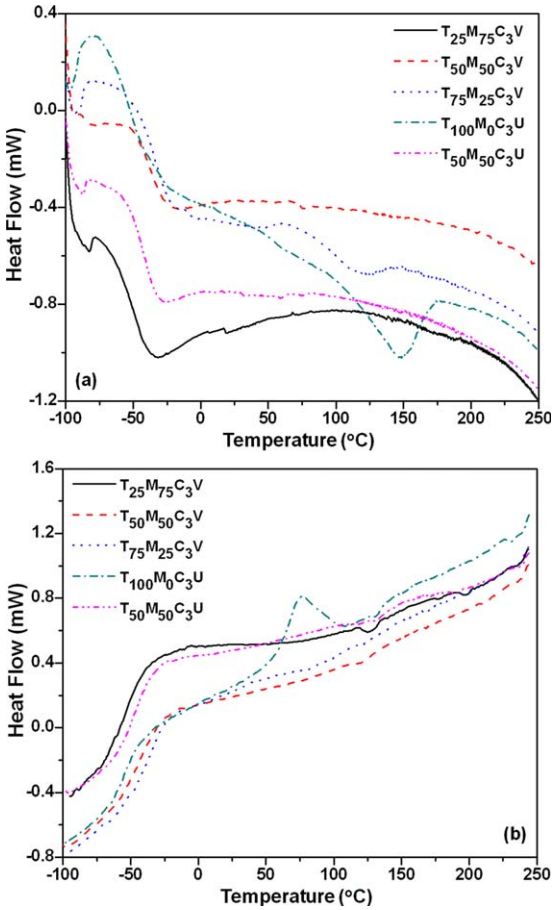

Figure 7. DSC thermograms for (a) second heating and (b) first cooling of samples. [Color figure can be viewed in the online issue, which is available at wileyonlinelibrary.com.]

centered at 150°C, which corresponds to the T_m of the crystalline domains of the hard segments ($T_{m(\text{hard})}$) of TPU matrix. The crystalline melting points of hard segments for $T_{25}M_{25}C_3V$ and $T_{50}M_{50}C_3V$ are completely disappeared, because the regular ordered structures of the crystalline hard segments are completely ruptured by the dynamic vulcanization process due to the creation of crosslinked polymeric network structures, high shearing action during melt blending, and development of interphase attractions of polyurethane matrix with organoclays via hydrogen bonding. The $T_{75}M_{25}C_3V$ showed a small broad melting peak, which reallocated to the lower temperature of around 125°C because of the presence of small ordered crystalline parts in hard-segments. This is due to the sufficient hindrance imposed through dynamic vulcanization process on hard segments to form large crystalline region. The heat of crystallization ($\Delta H_{c(\text{hard})}$) measured from the area associated with the hard segment crystalline melting peak substantially decreased for $T_{75}M_{25}C_3V$ in comparison with the $T_{100}M_0C_3U$, which notified that the degree of crystallinity is reduced to a large extent by the addition of more elastomeric MPU matrix. It is also concluded that the mixing of MPU with TPU at high temperature and large shearing force caused disruption of crystalline region that supported the early recovery of the regular molecular hard segment into its original regular crystalline state.[22] The melting point of simple TPU/MPU blend nanocomposite is disappeared due to the destruction of ordered regular structures in the polyurethane matrix resulted from the interference of MPU matrix on the segmental orientation or alignment of spherulite and crystallites within the hard segments.

The DSC thermograms for cooling cycle of samples are shown in Figure 7(b). The TPU nanocomposite ($T_{100}M_0C_3U$) illustrated a broad exothermic peak centered at 77°C, which is ascribed to the T_c of the hard domains ($T_{c(\text{hard})}$) of TPU matrix. This may be assisted by the positive nucleating effect imparted by the uniformly dispersed organoclays within TPU matrix. The $T_{c(\text{hard})}$ for dynamic vulcanized TPU/MPU blend nanocomposites are completely disappeared because of the materialization of the three-dimensional polymeric network structures that came into picture via dynamic vulcanization of the elastomeric MPU matrix, which restricted the initiation of the crystalline phase within the hard domain of the TPU matrix. The simple TPU/MPU blend nanocomposite also lost the $T_{c(\text{hard})}$ that is due to the formation of cocontinuous macrostructure of TPU/MPU blend matrix, which restricted the molecular chain mobility, thus hindered the smooth growth of the crystallites in the hard segments.[19]

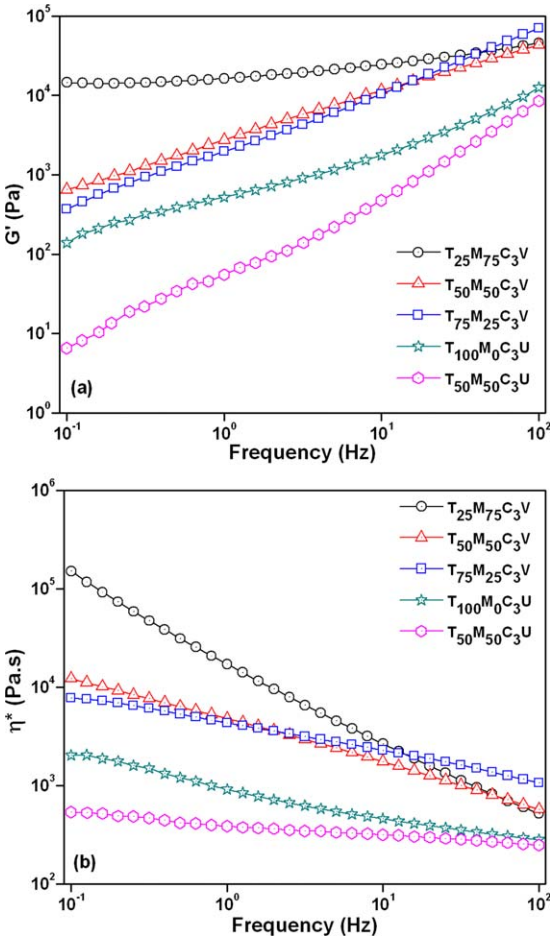

Figure 8. Frequency dependence of (a) storage modulus (G') and (b) complex viscosity (η^*) of samples. [Color figure can be viewed in the online issue, which is available at wileyonlinelibrary.com.]

Rheological Properties

Dynamic melt rheological property was investigated to observe the melt processability of the prepared nanocomposites. The frequency dependence of both storage modulus (G') and complex viscosity (η^*) of all samples in the molten state are shown in Figure 8(a,b), respectively. The G' increased with increasing applied angular frequency for all samples, but the slopes at the terminal region varied with blend composition and dynamic vulcanization process. TPU nanocomposite ($T_{100}M_0C_3U$) showed higher G' than TPU/MPU blend nanocomposite ($T_{50}M_{50}C_3U$) at lower frequency region, which indicates a more pronounced solid like behavior of the $T_{100}M_0C_3U$ than $T_{50}M_{50}C_3U$.[45–47] As discussed above, the clay nanoparticles have higher affinity for TPU than MPU, and the clay nanolayers are more finely dispersed in $T_{100}M_0C_3U$ than in $T_{50}M_{50}C_3U$. Thus, formation of filler network is more pronounced in $T_{100}M_0C_3U$ than in $T_{50}M_{50}C_3U$, which caused higher G' with lower terminal region slope of $T_{100}M_0C_3U$ than that of $T_{50}M_{50}C_3U$. Dynamically vulcanized blend nanocomposites showed higher G' and lower terminal region slope than TPU nanocomposite and TPU/MPU blend nanocomposite. With increasing MPU content in the dynamically vulcanized blends, G' increased and slope of terminal region decreased. Such trend in the dynamically vulcanized nanocomposites reflects crosslinked MPU domains, which hindered the dynamic relaxation process of the samples.

Plot of η^* versus frequency as in Figure 8(b) revealed that all samples exhibit a shear thinning behavior i.e., η^* decreased with increase in applied frequency at higher frequency region, which originated from the decreased resistance to flow against shear stress.[48] The viscosity level increases with decreasing the TPU fraction in the TPU/MPU blend systems. TPU nanocomposite ($T_{100}M_0C_3U$) has higher η^* than TPU/MPU blend nanocomposite ($T_{50}M_{50}C_3U$) and the $T_{100}M_0C_3U$ showed more pronounced shear thinning effect than $T_{50}M_{50}C_3U$. This is also in agreement with other results that TPU has a higher affinity with clay than MPU, and clays are more finely dispersed in TPU matrix than in TPU/MPU blend matrix. Dynamically vulcanized TPU/MPU blend nanocomposites showed higher η^* values and higher shear thinning effect than TPU nanocomposite and simple TPU/MPU blend nanocomposite. With increasing MPU content in the dynamically vulcanized TPU/MPU blend, η^* increased with higher shear thinning effect. Such trend in the dynamically vulcanized nanocomposites reflects crosslinked MPU domains, which increased the resistance to flow under applied frequency. This is also due to increase in interfacial interactions between TPU and MPU phases with increase in MPU content because of the higher surface area of the rubbery MPU phase.[22]

CONCLUSIONS

Polymer nanocomposites based on dynamically vulcanized TPU/MPU blend, simple TPU/MPU blend, and TPU with 3 phr organoclay were prepared by a melt mixing process. FTIR and morphology studies revealed that the interfacial interactions between the organoclays and matrix increased with TPU content in the blend and by a dynamic vulcanization process, and thereby, the degree of dispersion of the organoclay in the matrix was improved by the same factors. Higher reinforcement effect of the organoclay can be seen in the blends with higher TPU content and dynamically vulcanized blend. Dynamically vulcanized nanocomposite samples exhibited low hardness and high permanent set, which is attributed to the good elastomeric behavior of the TPU/MPU blend matrix. Thermal stability of the TPU/MPU blend matrix is well recovered by the dynamic vulcanization process and uniform dispersion of organoclays. Melt rheological analysis revealed that all nanocomposite samples showed solid-like behavior as well as a shear thinning behavior, which was more prominent in the dynamically vulcanized blend nanocomposites with higher TPU content.

ACKNOWLEDGEMENT

This work is supported by the research fund of Hanyang University (HY-2012-P). The postdoctoral research fellowship provided by Hanyang University is gratefully acknowledged by one of the author (A. K. Barick).

REFERENCES

1. Ray, S. S.; Okamoto, M. *Prog. Polym. Sci.* **2003**, *28*, 1539.
2. Pavlidou, S.; Papaspyrides, C. D. *Prog. Polym. Sci.* **2008**, *33*, 1119.
3. Cho, J. W.; Paul, D. R. *Polymer* **2001**, *42*, 1083.
4. Paul, D. R.; Robeson, L. M. *Polymer* **2008**, *49*, 3187.
5. Babu, R. R.; Naskar, K. *Adv. Polym. Sci.* **2011**, *239*, 219.
6. De, S. K.; Bhowmick, A. K. Thermoplastic Elastomers from Rubber-Plastic Blends; Ellis Horwood: New York, **1990**.
7. Coran, A. Y.; Patel, R. P. In Thermoplastic Elastomers; Holden, G., Kricheldorf, H. R., Quirk, R. P., Eds.; Carl Hanser Verlag: Munich, **2004**; Chapter *7*, pp 143–181.
8. l'Abee, R.; Goossens, H.; van Duin, M. *Polymer* **2008**, *49*, 2288.
9. Lee, K. Y.; Goettler, L. A. *Polym. Eng. Sci.* **2004**, *44*, 1103.
10. Mishra, J. K.; Kim, G.-H.; Kim, I.; Chung, I.-J.; Ha, C.-S. *J. Polym. Sci. Part B: Polym. Phys.* **2004**, *42*, 2900.
11. Mishra, J. K.; Kim, I.; Ha, C.-S.; Ryou, J.-H.; Kim, G.-H. *Rubber Chem. Technol.* **2005**, *78*, 42.
12. Mishra, J. K.; Hwang, K.-J.; Ha, C.-S. *Polymer* **2005**, *46*, 1995.
13. Wu, T.-M.; Chu, M.-S. *J. Appl. Polym. Sci.* **2005**, *98*, 2058.
14. Mirzazadeh, H.; Katbab, A. A. *Polym. Adv. Technol.* **2006**, *17*, 975.
15. Chatterjee, K.; Naskar, K. *Polym. Eng. Sci.* **2008**, *48*, 1077.
16. Siengchin, S.; Karger-Kocsis, *J. Compos. A: Appl. Sci. Manufact.* **2010**, *41*, 768.
17. Saikrasun, S.; Amornsakchai, T. *J. Polym. Res.* **2012**, *19*, 9750.
18. Munusamy, Y.; Ismail, H.; Mariatti, M.; Ratnam, C. T. *J. Reinf. Plast. Compos.* **2008**, *27*, 1925.
19. Pichaiyut, S.; Nakason, C.; Vennemann, N. *Iran. Polym. J.* **2012**, *21*, 65.
20. Minnath, M. A.; Unnikrishnan, G.; Purushothaman, E. *J. Membr. Sci.* **2011**, *379*, 361.

21. Kalkornsurapranee, E.; Nakason, C.; Kummerlöwe, C.; Vennemann, N. *J. Appl. Polym. Sci.* **2013**, *128*, 2358.

22. Pichaiyut, S.; Nakason, C.; Kummerlöwe, C.; Vennemann, N. *Polym. Adv. Technol.* **2012**, *23*, 1011.

23. Dhamodharan, R.; Maiti, P.; Radhakrishnan, G. *Polym. Plast. Technol. Eng.* **2008**, *47*, 1081.

24. Tan, J.; Ding, Y. M.; He, X. T.; Liu, Y.; An, Y.; Yang, W. M. *J. Appl. Polym. Sci.* **2008**, *110*, 1851.

25. Kotal, M.; Srivastava, S. K.; Bhowmick, A. K. *Polym. Int.* **2010**, *59*, 2.

26. Susteric, Z.; Dimitrievski, I. *Int. J. Polym. Mater. Polym. Biomater.* **2003**, *52*, 527.

27. Mahmood, N.; Khan, A. U.; Ali, Z.; Khan, M. S.; Haq, A.-U.; Stöckelhuber, K. W.; Gohs, U.; Heinrich, G. *J. Appl. Polym. Sci.* **2012**, *123*, 3635.

28. Abraham, T.; Abdou-Sabet, S.; Ouhadi, T.; Barber, N. (Advanced Elastomer Systems LP) U.S. Patent 6,207,752 (**2001**).

29. Gopi, J. A.; Nando, G. B. *J. Elastom. Plast.* **2012**, *44*, 189.

30. Rajan, K. P.; Al-Ghamdi, A.; Ramesh, P.; Nando, G. B. *J. Polym. Res.* **2012**, *19*, 9872.

31. Lei, C.-H.; Li, S.-L.; Xu, R.-J.; Xu, Y.-Q. *J. Elastom. Plast.* **2012**, *44*, 563.

32. Wu, J.-H.; Li, C.-H.; Wu, Y.-T.; Leu, M.-T.; Tsai, Y. *Compos. Sci. Technol.* **2010**, *70*, 1258.

33. Gan, L.-M.; Ni, H.-Y.; Zhou, Y.-J.; Chen, J. *J. Macromol. Sci. B: Phys.* **2011**, *50*, 1491.

34. Mishra, J. K.; Kim, I.; Ha, C.-S. *Macromol. Rapid Commun.* **2004**, *25*, 1851.

35. Barick, A. K.; Jung, J.-Y.; Choi, M.-C.; Chang, Y.-W. *J. Appl. Polym. Sci.* **2013**, *129*, 1405.

36. Pattanayak, A.; Jana, S. C. *Polymer* **2005**, *46*, 3275.

37. Tien, Y. I.; Wei, K. H. *Polymer* **2001**, *42*, 3213.

38. Kuan, H. C.; Ma, C. C. M.; Chuang, W. P.; Su, H. Y. *J. Polym. Sci. Part B: Polym. Phys.* **2004**, *43*, 1.

39. Pospíšil, M.; Čapková, P.; Měřínská, D.; Maláč, Z.; Šimoník, J. *J. Colloid Interface Sci.* **2001**, *236*, 127.

40. Fornes, T. D.; Yoon, P. J.; Keskkula, H.; Paul, D. R. *Polymer* **2001**, *42*, 9929.

41. Dan, C. H.; Lee, M. H.; Kim, Y. D.; Min, B. H.; Kim, J. H. *Polymer* **2006**, *47*, 6718.

42. Tavakoli, M.; Katbab, A. A.; Nazockdast, H. *J. Appl. Polym. Sci.* **2012**, *123*, 1853.

43. Kalkornsurapranee, E.; Vennemann, N.; Kummerlöwe, C.; Nakason, C. *Iran. Polym. J.* **2012**, *21*, 689.

44. Tien, Y. I.; Wei, K. H. *J. Appl. Polym. Sci.* **2002**, *86*, 1741.

45. Krishnamoorti, R.; Yurekli, K. *Curr. Opin. Colloid Interface Sci.* **2001**, *6*, 464.

46. Aubry, T.; Razafinimaro, T.; Médéric, P. *J. Rheol.* **2005**, *49*, 425.

47. Médéric, P.; Razafinimaro, T.; Aubry, T. *Polym. Eng. Sci.* **2006**, *46*, 986.

48. Huitric, J.; Ville, J.; Médéric, P.; Moan, M.; Aubry, T. *J. Rheol.* **2009**, *53*, 1101.